

Morphology-dependent crossover effects in heterogeneous nucleation of peritectic materials studied via the phase-field method for Al–Ni

This article has been downloaded from IOPscience. Please scroll down to see the full text article.

2009 J. Phys.: Condens. Matter 21 464105

(<http://iopscience.iop.org/0953-8984/21/46/464105>)

View [the table of contents for this issue](#), or go to the [journal homepage](#) for more

Download details:

IP Address: 129.252.86.83

The article was downloaded on 30/05/2010 at 06:02

Please note that [terms and conditions apply](#).

Morphology-dependent crossover effects in heterogeneous nucleation of peritectic materials studied via the phase-field method for Al–Ni

R Siquieri and H Emmerich

Center for Computational Engineering Science and Institute of Minerals Engineering,
RWTH Aachen University, D-52056 Aachen, Germany

E-mail: emmerich@ghi.rwth-aachen.de

Received 7 May 2009, in final form 18 August 2009

Published 27 October 2009

Online at stacks.iop.org/JPhysCM/21/464105

Abstract

The application of phase-field modeling to nucleation as a phenomenon at the nanoscale is justified, if one takes into account the great success of continuum approaches in nanofluidics as proven by the many comparisons to experiments. Employed in this manner it provides an approach allowing us to account for effects of the physical diffuseness of a nucleus' interface and thereby go beyond classical nucleation theory (Gránásy and James 2000 *J. Chem. Phys.* **113** 9810; Emmerich and Siquieri 2006 *J. Phys.: Condens. Matter* **18** 11121). Here we extend the focus of previous work in this field and address the question of how far the phase-field method can also be applied to gain further insight into nucleation statistics, in particular the nucleation prefactor appearing in the nucleation rate. In this context we describe in detail a morphology-dependent crossover effect noticeable for the nucleation rate at small driving forces.

1. Introduction

Nucleation is a complex fluctuation phenomenon. Atomistic simulations performed by Swope and Andersen [1] and Wolde and Frenkel [2] reveal that, even during homogeneous crystal nucleation in a single-component liquid, several local atomic arrangements (bcc, fcc, hcp, icosahedral) compete, of which oftentimes a metastable phase becomes dominant. For multi-component and phase alloys the complexity increases, as the composition of nuclei enters as an extra state variable. Nevertheless, the development of approaches towards multi-component nucleation is still based on the classical kinetic theory of nucleation, which had first been formulated by Farkas [3] and Becker and Döring for homogeneous nucleation, and was successively adopted for general first-order phase transformations in condensed matter physics by Turnbull and Fisher [4]. The approach relies on a set of master equations that consider only single-molecule attachment and detachment processes (a good approximation in the early stages of solidification). Analytical as well as numerical treatment of the problem indicates that, after a transient

period, steady state conditions are established, under which the nucleation rate, i.e. the net volumetric formation rate of critical fluctuations, can be expressed as

$$I = I_0 \exp\left(\frac{\Delta F^*}{k_B T}\right). \quad (1)$$

Here I_0 is the nucleation prefactor, which is assumed to be constant in classical theories [16]—an empirical assumption which is contradicted by recent theoretical studies in [17], which are themselves in accordance with experiments in organic crystals. F^* is the free energy of critical fluctuations, while k_B and T are the Boltzmann factor and the temperature, respectively. In determining the free energy of the heterophase fluctuations, the classical nucleation theory relies on the droplet model (introduced by Gibbs for studying phase stability), which views the heterophase fluctuations as spherical crystals, which free energy is expressed in terms of their radius R , the volumetric free energy difference $\Delta g (< 0)$ between bulk and crystal and the undercooled liquid, as well as

the interfacial free energy γ :

$$F = \left(\frac{4\pi}{3}\right) R^3 \Delta g + 4\pi R^2 \gamma. \quad (2)$$

Equation (2) reveals that a maximum of $F^* = (16\pi/3)\gamma^3/\Delta g^2$ is reached at the critical radius $R^* = -2\gamma/\Delta g$.

The adaptation of this classical droplet model to heterogeneous nucleation has been reviewed by Christian [5]. The most commonly discussed model in this context is the spherical cap model taking into account the free energy reduction due to the creation of a triple junction line between the nucleating solid, the liquid and a pre-existing solid phase (container wall, foreign particle, primary phase), which acts as a substrate. Under such conditions only a fraction of the homogeneous nucleus needs to be formed by random fluctuations, a phenomenon that reduces the height of the nucleation barrier. For a planar interface, the critical fluctuation is a spherical cap, whose size is determined by the contact angle θ between the solid–substrate and liquid–solid interfaces. The latter—in turn—is fully determined by the free energies of the solid–liquid, solid–substrate and liquid–substrate interfaces. Under such conditions, the ratio of the free energies of the heterogeneous and homogeneous nuclei is given by the catalytic potency factor:

$$f(\theta) = (2 + \cos\theta)(1 - \cos\theta)^2/4. \quad (3)$$

The drawbacks of classical nucleation theory emerge from those of the droplet model, which rely on the thermodynamic properties of the macroscopic bulk phase, when calculating the free energy of near-critical clusters. According to the experiments by Howe [6] and Huisman *et al* [7] and computer simulations, as reviewed by Laird and Haymet [8], the crystal–liquid and crystal–glass interfaces are diffuse on the molecular scale, extending over several molecular layers, with an interface thickness comparable to the size of critical fluctuations. This invalidates the main assumption of the droplet model that the interface thickness is negligible with respect to the size of the fluctuations. As a consequence two new challenges emerge.

- (i) To derive a kinetic theory that incorporates the differences in the diffusion of the individual species.
- (ii) To develop models that include the dependence of the Gibbs free energy and interface free energy on cluster composition and cluster size for multi-component alloys.

Reviews by Gunton [9], Gránásy and James [10] and Oxtoby [11] give a survey on these new developments. Moreover, focusing on the heterogeneous nucleation event tied to the nucleation of a new nucleus on the surrounding system's wall, first steps were set by Castro [12] and Gránásy *et al* [13]. Castro [12] introduced walls into a single-order-parameter model (one-component case) by assuming a no-flux boundary condition at the interface ($\mathbf{n}\nabla\phi = 0$, where \mathbf{n} is the normal vector of the wall), which results in a contact angle of 90° at the wall–solid–liquid triple junction. Subsequently Langevin noise is introduced to model nucleation. Following a similar

route, Gránásy *et al* [13] introduced chemically inert surfaces ($\mathbf{n}\nabla\phi = 0$ and $\mathbf{n}\nabla c = 0$ at the wall perimeter) into a binary phase-field theory while incorporating an orientation field, and performed simulations to address heterogeneous nucleation on foreign particles, at rough surfaces and in confined space (porous matter and channels). This work has recently been extended by the author and others in [14, 15]. Here we extend the focus of previous work in this field and address the question of how far it can also be applied to gain further insight into nucleation statistics, in particular the nucleation prefactor appearing in the nucleation rate. In this context we describe in detail a morphology-dependent crossover effect noticeable for the nucleation rate at small driving forces. We apply our study to Al–Ni. This allows us to exploit our own previous joint theoretical–experimental studies on this system [19] which enabled us to calibrate our phase-field model quantitatively. That joint study focuses on growth phenomena as the ones accessible with the experimental techniques employed in that reference. The nucleation event, in particular the individual one, is in contrast hard to access in such metallic systems. The studies we report here allow us to extend the understanding we obtained for specific growth phenomena in peritectic Al–Ni to nucleation therein and thus obtain a comprehensive picture about the initial stages of growth in Al–Ni. For details regarding the calibration the reader is referred to [19]. Furthermore our work is based on our own work in the field of heterogeneous nucleation involving the phase-field method in which we could demonstrate that the approach is well suited to access nucleation barriers [18]. Here we go a step further and focus on comparison to the results of Liu [17] on the question of what understanding it allows us to extract regarding the kinetic prefactor arising in the nucleation rate.

To show how the phase-field method can be employed to questions of nucleation statistics related to the kinetic prefactor I_0 and the study in [17]¹ we proceed as follows: we will first briefly describe our methodological approach in section 2 of this paper. We will then—in section 3—proceed to our precise studies of the nucleation rates in Al–Ni, which allow us to shed new light on the contradictory claim arising from the paper by Liu in comparison to classical theories (see, e.g., [16]). One result which we report in more detail in this context is a morphology-dependent crossover of the nucleation rate found at high undercoolings *independent* of I_0 . Finally we conclude with a discussion of our results, their interpretation and the outlook in section 4.

2. Brief review of our model

2.1. Phase-field modeling of peritectic material systems

In this section we brief describe the phase-field formulation employed to compute heterogeneous nucleation. We use an

¹ Note that the focus of that study is on the nucleation of seed phases in general rather than only properitectic ones combined with the question of what cases true homogeneous nucleation can occur in comparison to heterogeneous nucleation. What is analogous to our studies is that, in this context, the effect of the radius of a seed grain on resulting nucleation energies and corresponding nucleation rates is investigated, revealing similar crossover effects as we see them in our study, and used to claim the form of the kinetic prefactor I_0 in a way that does not agree with our studies (for details see section 3).

isothermal version of the model described in [19]. For further details of the model see [19, 23]. The starting point of our phase-field modeling approach for heterogeneous nucleation is the free energy functional of a representative volume of the investigated material system. This free energy functional is given by the volume integral

$$\mathcal{F} = \int_V \left\{ \frac{W(\theta)^2}{2} \sum_i (\nabla p_i)^2 + \sum_i p_i^2 (1 - p_i)^2 + \tilde{\lambda} \left[\frac{1}{2} \left[c - \sum_i A_i(T) g_i(\vec{p}) \right]^2 + \sum_i B_i(T) g_i(\vec{p}) \right] \right\} dV, \quad (4)$$

where $W(\theta)$ depends on the orientation of the interface and $\tilde{\lambda}$ is a constant. The function g_i couples the phase field to the concentration and the temperature [19].

The coefficients $A_i(T)$ and $B_i(T)$ define the equilibrium phase diagram [23]:

$$A_i(T) = c_i \mp (k_i - 1)U, \quad A_L = 0,$$

$$B_i(T) = \mp A_i U \quad B_L = 0,$$

where $U = (T_p - T)/(|m_i| \Delta C)$ is the dimensionless undercooling, k_i are the partition coefficients, and A_L and B_L are the corresponding liquid coefficients.

As described in [19] we use three phase fields $p_i \in [0, 1]$, where p_1 labels the properitectic phase, p_2 the peritectic phase and p_3 the liquid phase, represented by $\vec{p} \equiv (p_1, p_2, p_3)$.

Their dynamics are derived from the free energy functional \mathcal{F} :

$$\tau \frac{\partial p_i}{\partial t} = -\frac{1}{H} \frac{\delta \mathcal{F}}{\delta p_i}, \quad (5)$$

where τ is a relaxation time.

The concentration field is given by

$$\frac{\partial c}{\partial t} = \vec{\nabla} \cdot \left(D(\vec{p}) \vec{\nabla} \frac{\delta \mathcal{F}}{\delta c} \right), \quad (6)$$

where $D(\vec{p})$ is a phase-dependent diffusivity.

Model equations (5) and (6) were solved numerically in the same way as described in [19].

2.2. Investigating heterogeneous nucleation in peritectic material systems via the phase-field method

In solidification experiments the final microstructure is determined by both the peritectic growth dynamics as well as the microstructure growth kinetics. Therefore, for a full quantitative comparison with experiments, it is essential to analyze the heterogeneous nucleation kinetics of the above peritectic material system as well. For such a system a nucleation event arises as a critical fluctuation, which is a non-trivial time-independent solution of the governing equations we can derive from the underlying free energy functional. Our derivation follows the standard variational procedure of phase-field theory (for a review see, e.g., [21] and references therein). Solving equations (4)–(6) numerically under boundary conditions that prescribe bulk liquid properties

far from the fluctuations ($p_i \rightarrow 1$ and $c \rightarrow c_\infty$ at the outer domain boundaries) and zero field gradients at the center, one obtains the free energy of the nucleation event as

$$\Delta F^* = \mathcal{F} - \mathcal{F}_0. \quad (7)$$

Here \mathcal{F} is obtained by numerically evaluating the integration over \mathcal{F} after having the time-independent solutions inserted, while \mathcal{F}_0 is the free energy of the initial liquid. Based on (7) the corresponding nucleation rate can be calculated as follows:

$$I = I_0(R_s) \exp\{-\Delta F^*/kT\}, \quad (8)$$

where R_s denotes the radius of the seed grain, which is, in our case, the primary, properitectic grain. Notice that this deviates from the classical form given in the above equation (1) in the sense that I_0 does not necessarily need to be constant any longer. Rather we have set I_0 to $I_0(R_s)$ to indicate that in the following we will test different forms of I_0 : (a) the classical, constant form, thus assuming an R_s -independent form for I_0 and (b) the R_s -dependent one given by Liu in [17] as follows:

$$I_0(R_s) = 4\pi a(R_s)^2 N^0 f''(m, x) [f(m, x)]^{1/2} B \quad (9)$$

with

$$f(m, x) = 1/2 + 1/2 \left(\frac{1.0 - xm}{w} \right)^3 + 1/2x^3 \left[2.0 - 3 \left(\frac{x - m}{w} \right) + \left(\frac{x - m}{w} \right)^3 \right] + \frac{3}{2} mx^2 \left(\frac{x - m}{w} - 1 \right)$$

where $w = (1 + x^2 - 2xm)^{1/2}$, $x = R_s/r_c$ and r_c is the critical size of the nucleating phase.

This allows us to shed new light on the contradictory issue whether (a) or (b) is the more appropriate form.

3. Reaccessing I_0 at the example of Al–Ni

Focusing on Al–Ni allows us to make use of our own results obtained in tight collaborative experimental–theoretical studies of that system [19]. To our knowledge these are the first systematic studies of nucleation energies and related nucleation rates in Al–Ni. All the calculations are performed for the isothermal case and for an initial alloy composition $c_\infty = 23$ mol% with alpha concentration $c_\alpha = 35$ mol% and beta concentration $c_\beta = 25$ mol%. We use a linearized version of the Al–Ni phase diagram and choose $m_\alpha = 6642.8$ K/mol% and $m_\beta = 19000.0$ K/mol%. The partition coefficients are taken as $k_\alpha = k_\beta = 1.0$. The diffusion constant in the liquid phase is taken as $D_L = 1 \times 10^{-9}$ m² s⁻¹ and in the solid $D_S = 0$. We assume equal surface tension in both solid phases of value $\sigma_{\beta,L} = \sigma_{\alpha,L} = 0.09$ J m⁻²; moreover $\sigma_{\alpha,\beta} = 0.068$ J m⁻². The undercooling ΔT was varied from 0.03 to 0.9. We perform our tests in a simulation box of 300×300 grid points, corresponding to a sample of $80 \mu\text{m} \times 80 \mu\text{m}$. With these parameter configurations we studied the cases where the radius $R_s = 20, 30$ and 40 grid points.

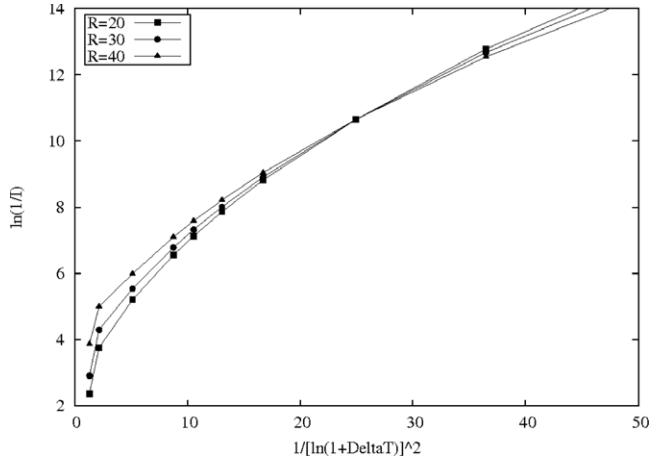


Figure 1. $\ln(1/I)$ versus $1/[\ln(1 + \Delta T)]^2$ to display the dependence of I_0 on the driving force ΔT . Nucleation rates are evaluated based on our phase-field approach assuming a classical, i.e. constant, I_0 .

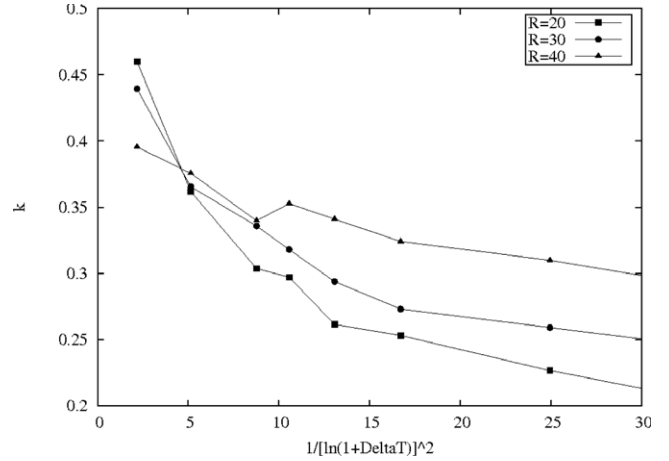


Figure 3. Integrated curvature of the phase-field versus $1/[\ln(1 + \Delta T)]^2$.

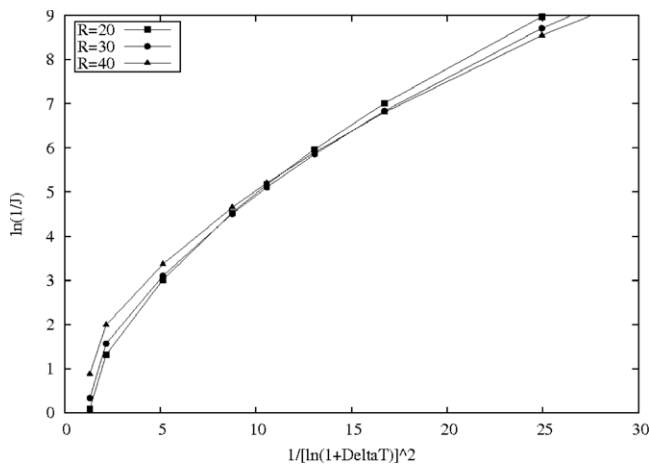


Figure 2. The same as in figure 1: however, nucleation rates are evaluated based on our phase-field approach assuming an R_s -dependent value for I_0 as given by equation (19) of [17].

More precisely we have been interested in the dependence of the nucleation rate on the radius of the underlying seed phase R_s . For this we could already see in our previous work on Fe–Ni [18] that the nucleation rate is generally larger for (low curved) seed nuclei of larger radius and also on non-faceted compared to faceted nuclei if we nucleate in the corner of the facet. This has also been found in Monte Carlo studies and qualitatively for Nd–Fe–B.

At high driving forces (left part of figures 1–3), however, we see a crossover effect, i.e. nucleation on stronger curved (and thus smaller) seed nuclei becomes more favorable. This is depicted in this paper for Al–Ni in figure 1. In our calculations underlying that figure we follow the classical nucleation theory assuming a constant I_0 . The crossover effect on which we focus here can also be found in figure 4 of [17]². In [17],

² Note that the driving force there is rather the supersaturation than the temperature. The thermodynamic equivalence of these two in their role as the main driving force for microstructure evolution has been explained in detail in [21, 20, 24].

however, the author assumes an R_s -dependent form of I_0 . With this form his theoretical studies are in good agreement with experiments in organic crystals. This leads Liu to the conclusion that a non-constant but rather the R_s -dependent form of I_0 given in equation (19) of his article [17] should be a more correct form of I_0 than the classically assumed one. Our studies summarized in figure 1, however, reveal that in our studies such a crossover is also observable if we calculate the nucleation rate based on the nucleation energies determined via our phase-field simulations simply following the classical relation given by equation (1) with constant I_0 . In fact, the appearance of the crossover as such—and with it the appearance of the different nucleation regimes Liu identifies—is independent of the precise form of I_0 , as we verified by repeating our calculations with the kinetic prefactor given by equation (19) of [17]. These calculations are depicted in figure 2. If we compare figures 1 and 2 we can see that the respective curves deviate little quantitatively and hardly qualitatively. Thus the appearance of the crossover and the different nucleation regimes which can be deduced from that crossover do not allow us to claim a precise form of I_0 different from the classical one according to our studies. In this context one should note, too, that according to our studies the crossover as such should already appear in that regime of the nucleation rate curves, where these are still curved logarithm-like as shown in our figures, rather than after the turning point at still higher undercoolings as implied by [17].

Based on additional phase-field simulation studies we are also able to understand the physical origin of that crossover, which appears to be the *interface diffusivity*, which changes with undercooling. As measured for that interface diffusivity, i.e. the interface width, which at the critical point investigated here corresponds to the correlation length [22], we evaluated the integrated curvature of the phase field and plotted it versus temperature³. This plot is shown in figure 3. It displays an analogous crossover: for small radii of the seed nucleus

³ The integrated curvature is calculated according to $\kappa(p_1) = \int_V -\nabla(\nabla p_1/|\nabla p_1|) dV$. Thus it gives a measure for the interface width of the relevant phase-field order parameter.

the integrated curvature of the phase field is larger at high undercoolings than that of the larger radii. Since the interfacial width is inversely proportional to the integrated curvature this implies, too, that in turn the interfacial width is larger for the larger radii at high undercoolings. This yields an explanation for the observed crossover in the nucleation rate: small seed nuclei with large curvature are generally favorable for the nucleation rate on such seeds, since this comes along with an increased surface area exposed to the nucleating phase (or, more precisely, an improved surface to volume ratio compared to a less curved substrate). However, the same accounts for an enlarged surface area due to an enlarged interfacial width—which Liu calls ‘effective surface embryos’. Now the decrease of the interfacial width, which the small nuclei undergo at smaller driving forces (right part of the figures), obviously overrides the first effect and thus helps to understand why at smaller undercoolings nucleation becomes more favorable on the seed grains with larger radii. In the sense that Liu conjectures a similar reason for the crossover in his studies, namely the increased ‘effective surface embryos’, our studies reconcile with his from the point of view of the physical interpretation. Nevertheless our studies question his R_s -dependent form of I_0 , as well. Certainly there is demand for research focusing on a more precise form of I_0 , which goes beyond classical nucleation theory. If there is more high accuracy experimental data available of nucleation rates in particular within the high undercooling regime, the phase-field approach, which we present here, can contribute to that open issue: as demonstrated here it allows us to test different forms of I_0 and thus could—in close comparison to experiments—help to identify ideal ones beyond the classical theories.

4. Summary and outlook

To summarize, in this paper we have employed the phase-field approach to determine nucleation energies of heterogeneously nucleating peritectic material systems, which we introduced earlier in [18], for a systematic study of heterogeneous nucleation in Al–Ni with a special focus on (a) a crossover in the nucleation rates at high undercoolings and (b) on the kinetic prefactor I_0 . We can explain point (a) based on our phase-field approach as a morphology-dependent crossover of the correlation length. Details are given in the previous section. For (b) we referred to previous work by Liu [17], who identified the same crossover and corresponding different regimes of heterogeneous nucleation via a different theoretical approach. Since he found experimental agreement for his

studies and furthermore, since he assumed an R_s -dependent form of I_0 in his investigations, he claimed this form to be more appropriate than the classical constant one. This claim, however, is contradictory to our studies, which identify the crossover based on the assumption of a constant I_0 . Moreover we can show that the crossover as such is independent of the two forms of I_0 , leaving the issue of an I_0 beyond classical nucleation theory open at this point. If there is more high accuracy experimental data available of nucleation rates in particular within the high undercooling regime, the phase-field approach, which we follow here, can contribute to that open issue: as demonstrated here it allows us to test different forms of I_0 and thus could—in close comparison to experiments—help to identify ideal ones beyond the classical theories.

References

- [1] Swope W C and Andersen H C 1990 *Phys. Rev. B* **41** 7042
- [2] ten Wolde P R and Frenkel D 1999 *Phys. Chem. Chem. Phys.* **1** 2191
- [3] Farkas J 1927 *Z. Phys. Chem.* **38** 236
- [4] Turnbull D and Fisher J C 1949 *J. Chem. Phys.* **17** 71
- [5] Christian J W 1975 *The Theory of Transformations in Metals and Alloys* (Oxford: Oxford University Press)
- [6] Howe J M 1996 *Phil. Mag. A* **74** 761
- [7] Huisman W J, Peters J F, Zwaneburg M J, de Vries S A, Derry T E, Abernathy D and van der Veen J F 1997 *Nature* **390** 379
- [8] Laird B B and Haymet A D 1992 *J. Chem. Rev.* **92** 1819
- [9] Gunton J D 1999 *J. Stat. Phys.* **95** 903
- [10] Gránásy L and James P F 2000 *J. Chem. Phys.* **113** 9810
- [11] Oxtoby D W 1991 *Liquids, Freezing and Glass Transition* (Amsterdam: Elsevier)
- [12] Castro M 2003 *Phys. Rev. B* **67** 035412
- [13] Gránásy L, Pusztai T and Warren J A 2009 at press
- [14] Gránásy L, Pusztai T, Saylor D and Warren J A 2009 *Phys. Rev. Lett.* **98** 035703
- [15] Warren J A, Pusztai T, Környei L and Gránásy L 2009 *Phys. Rev. B* **79** 1
- [16] Kelton K F 1991 *Solid State Phys.* **45** 75
- [17] Liu X Y 2000 *J. Chem. Phys.* **112** 9949
- [18] Emmerich H and Siquieri R 2006 *J. Phys.: Condens. Matter* **18** 11121
- [19] Siquieri R, Doernberg E, Schmid-Fetzer R and Emmerich H 2009 *J. Phys.: Condens. Matter* **21** 464112
- [20] Emmerich H 2003 *Contin. Mech. Thermodyn.* **15** 197
- [21] Emmerich H 2003 *The Diffuse Interface Approach in Material Science—Thermodynamic Concepts and Applications of Phase-Field Models* (Springer Monograph, Lecture Notes in Physics LNP m 73)
- [22] Das S K, Horbach J and Binder K 2009 *Phys. Rev. E* **79** 021602
- [23] Folch R and Plapp M 2005 *Phys. Rev. E* **72** 011602
- [24] Emmerich H 2008 *Adv. Phys.* **57** 1